Breaking Cycles: Saponification-Enhanced NMR Fingerprint Matching for the Identification and Stereochemical evaluation of cyclic lipodepsipeptides from natural sources

Penthip Muangkaew[§,[a]], Durga Prasad[[b]§], Vic De Roo[[b]], Yentl Verleysen[[a]], René De Mot[[c]], Monica Höfte[[d]], Annemieke Madder[[a]], Niels Geudens*[[b]] and José C. Martins*[[b]]

[a] Dr. Penthip Muangkaew, Dr. Yentl Verleysen, Prof. Dr. Annemieke Madder
Organic Biomimetic Chemistry Research Group, Department of Organic and Macromolecular Chemistry
Ghent University
Krijgslaan 281, S4bis, 9000 Ghent, Belgium

[b] Mr. Durga Prasad, Dr. Vic De Roo, Dr. Niels Geudens, Prof. Dr. José C. Martins
NMR and Structure Analysis Unit, Department of Organic and Macromolecular Chemistry
Ghent University
Krijgslaan 281, S4bis, 9000 Ghent, Belgium
E-mail: niels.geudens@ugent.be; jose.martins@ugent.be

[c] Prof. Dr. René De Mot
Centre for Microbial and Plant Genetics, Faculty of Bioscience Engineering
KULeuven
Kasteelpark Arenberg 20, 3001 Leuven, Belgium

[d] Prof. Dr. Monica Höfte
Laboratory of Phytopathology, Department of Plants and Crops
Ghent University
Coupure links 653, 9000 Ghent, Belgium

§ Shared first coauthorship

Supporting information for this article is given via a link at the end of the document.

Abstract: We previously described NMR based fingerprint matching using peptide backbone (CHα) resonances as a fast and reliable way to perform structural dereplication of *Pseudomonas* cyclic lipodepsipeptides (CLiPs). In addition, its combination with total synthesis of a small library of CLiPs was shown to afford unambiguous determination of the stereochemistry, further opening these compounds for structure-activity relationship studies and three-dimensional structure determination. However, the need to include on-resin macrocycle formation in the synthetic workflow results in considerable burden and limits universal applicability to CLiPs. Here we show that this drawback can be removed by first converting the native CLiP of interest into its linearized analogue via controlled hydrolysis of the depsi bond through saponification. By avoiding the macrocycle formation altogether, the required synthesis effort is strongly reduced as it now only requires production of linear peptide analogues. The NMR fingerprints of the linear peptide analogues display a sufficiently distinctive chemical shift fingerprint to act as effective discriminators. The approach is developed using viscosin group CLiPs and subsequently demonstrated on putisolvin, leading to a structural revision, and tanniamide, a newly isolated compound defining a new group in the *Pseudomonas* CLiP portfolio. These examples demonstrate the effectiveness of the saponification-enhanced approach that broadens applicability of NMR fingerprint matching for the determination of the stereochemistry of CLiPs.

Introduction

Cyclic lipodepsipeptides (CLiPs) are secondary metabolites synthesized non-ribosomally by bacteria from multiple genera including *Pseudomonas, Bacillus*, *Streptomyces* and *Burkholderia*. [1] They also contribute to the metabolite reservoir of many other, underexplored genera.[2] Their multifaceted biological activities play a key role in supporting their producer's lifestyle. They are involved in bacterial swarming, bacterial mobility and bacterial biofilm management.[3] They also contribute to plant-bacteria relationships that can lead to plant growth promoting activity and pathogen protection by direct antagonism or induced resistance.[1b, 4] Their well-documented antimicrobial activity makes them equally relevant for agricultural and pharmaceutical applications.[5] plant pathogenic microorganisms are a major cause of crop loss threatening global food security at a time where chemical pesticides are meeting pressures to be replaced by new biopesticides from natural sources.[6] Simultaneously, antimicrobial resistance is predicted to lead to a global human healthcare challenge in the absence of a robust and sustained development effort towards novel antibiotics and antifungals. Prime examples of the potential of CLiPs in addressing these pressing needs are provided by Serenade®, a *Bacillus* formulation with preventive antifungal action that relies on bacterial production of CLiPs, and the antibiotic Cubicin® based on daptomycin, a CLiP produced by *Streptomyces roseosporus* that is used to treat Gram-positive bacterial bacteremia and skin infections. From the perspective of fundamental and application-oriented research and development efforts, CLiPs therefore constitute an interesting source of novel bioactive compounds. Elucidating their structure is of vital

importance *en route* to understanding their properties and activity.[7]

The chemical blueprint of CLiPs results from their assembly by non-ribosomal peptide synthetases (NRPS) and features an oligopeptide sequence that is N-capped by an acyl chain and C-capped by ester bond formation with the hydroxyl group from a preceding amino acid residue in the sequence (all *Pseudomonas* CLiPs and iturin from *Bacillus*), or from the acyl chain (e.g. surfactin from *Bacillus*). Structural diversity arises from variations in total sequence length, macrocycle size and N-acyl fatty acid moiety. Furthermore, non-proteinogenic amino acids, featuring non-standard side-chains, a D-configuration, or a mixture thereof, are part of their make-up.[8] As a result, the determination of the planar structure alone, typically afforded by combined MS and NMR structure analysis methods, does not suffice for structure-activity relationship studies and three-dimensional structure determination of CLiPs, as both require knowledge of the full stereochemistry. To this end, bioinformatic prediction or chemical methods (e.g. Marfey's analysis), as recently discussed by Götze and Stallforth in their excellent review, should also be included.[9] However, depending on the particular CLiP at hand, these methods do not provide a failsafe pathway to the elucidation of stereochemistry. For instance, an increasing number of literature reports have documented cases where the presence of D-configured amino acids predicted from the analysis of the Epimerisation/Condensation (E/C) domains responsible for epimerization of L-configured precursors does not fit experimental data as a result of non-functional (epi-inactive)[10], or even intermittently functional[11] epimerization activity. Assuming L-amino acids are recruited by the NRPS, only the L-configuration of amino acids that are not exposed to epimerization activity during lipopeptide assembly on the NRPS, can be established with certainty.[10a] Chemical methods such as Marfey's analysis report on the configurational mix of amino acids, but require complete hydrolysis of the CLiP, thus removing any positional information regarding the distribution of amino acids present in both configurations. Therefore, when *in silico* and chemical methods are combined, multiple diastereomeric oligopeptide sequences may well fit all available data, leading the full structure elucidation process into a configurational dead end.[10a]

We recently demonstrated that the specific pattern of L/D-configurations along the sequence of a particular CLiP diastereoisomer creates a unique set of (CHα) $^{1}H;^{13}C$ chemical shifts. The stereochemistry of a particular CLiP is thus encoded in a unique NMR spectral fingerprint easily accessible from a ^{1}H-{^{13}C} HSQC spectrum and can be used for dereplication purposes of newly isolated CLiPs, even when the actual stereochemistry is yet to be established.[1a, 10a] We also showed that when the structure analysis pipeline described above results in multiple diastereomeric solutions, total synthesis of these followed by comparison of their respective (CHα) fingerprint with that of the natural compound provides a high fidelity procedure for the elucidation of CLiP stereochemistry. This obviously requires a convenient total synthesis pathway to the CLiP in question. In the case of *Pseudomonas* CLiPs, the common chemical blueprint has allowed us to use the synthesis route initially developed for the structure activity relationship studies of pseudodesmin A and other Viscosin (9:7) group members [12] to other CLiP groups in this genus, each synthesis requiring only minor modifications to the original scheme (Scheme 1a). The synthesis of small libraries of sequences combined with NMR fingerprinting subsequently allowed to elucidate the stereochemistry of representatives of the Bananamide (8:6), Xantholysin (14:8), and Entolysin (14:5) groups, whereby the (l:m) tag categorizes each group by the total number of residues in the oligopeptide sequence (l) and the macrocycle (m) respectively. We also showed a revision was in order for the stereochemistry of orfamide A (10:8), a conclusion also independently arrived at by Bando et al.[13]

Encouraged by these successes, we aimed to further streamline such approaches by reducing the synthetic footprint. Currently, our *Pseudomonas* CLiP synthesis starts (Scheme 1a – step 1) with sidechain anchoring to a chlorotrityl resin of a serine/threonine residue present in the native sequence as close as possible to the peptide's C-terminus. It is introduced with allylester protection of the carboxylgroup in view of later macrolactamisation (vide infra, Scheme 1a – step 5). Alternative side-chain anchoring approaches involving a glutamic or aspartic acid (using 2-CTC resin), glutamine/asparagine or a residue featuring a side-chain amine (using a rink linker to the 2-CTC resin) can also be used instead.[7a] Subsequently, the peptide sequence and N-capping acyl chain are introduced in a stepwise fashion using Fmoc/tBu-based solid-phase peptide synthesis (SPPS) (Scheme 1a – step 2), whereby, as it turns out, side-chain protection of the serine/threonine side-chain involved in the future depsi bond can be omitted. Next, (Scheme 1a – step 3) the ester bond is introduced by condensing the unprotected serine or threonine sidechain with the carboxyl of the future C-terminal residue. The latter is then extended (Scheme 1a – step 4) by the additional amino acids required between the anchored residue and the ester linked C-terminal residue, the final residue being introduced with an Alloc protecting group. The final peptide bond is then introduced by on-resin cyclisation, following simultaneous Allyl/Alloc deprotection using Pd chemistry (Scheme 1a – step 5). Acidic conditions then remove all protecting groups and induce cleavage causing the desired CLiP to be released from the resin (Scheme 1a – step 6). On resin cyclisation is preferred as it allows to involve the pseudo dilution phenomenon to favor intramolecular resin-bound reactions.[14] While already extensively applied to *Pseudomonas* CLiPs, the need to introduce an ester bond is more often than not accompanied by a number of complications. First, the on-resin esterification can be slow and prone to epimerization leading to undesirable stereoisomers, with loss of efficiency[13, 15] and ambiguity as a result. While this can be countered by using a preformed ester as building block, as demonstrated for the total synthesis of orfamide A (10:8), it depends on controlling N->O acyl migration during the Fmoc deprotection of the building block, which cannot be guaranteed.[13] In our hands for instance, application of this strategy to synthesis of viscosin proved less successful (Muangkaew, unpublished results). Additional problems that may impact the level of epimerization can also be caused by nearby bulky protecting groups, as demonstrated in the total synthesis of WLIP (9:7).[15]

Since these problems are connected to the often-challenging macrocycle formation, a Columbus' Egg solution would consist in avoiding its synthesis altogether if one is only interested in elucidating stereochemistry. Specifically, we conjectured that our NMR fingerprinting approach would still work when using the (CHα) fingerprint of linear diastereomeric sequences, obtained through classic SPPS, against the fingerprint of the linearized version of the natural compound, itself obtained through controlled hydrolysis of the depsi bond (Scheme 1b). This not only significantly decreases the synthetic burden involved but could

also expand its applicability to any cyclic (lipo)depsipeptide compound of undetermined stereochemistry. Indeed, it removes the effort of developing specifically tailored total synthesis routes for the desired macrocycle when the latter cannot be achieved through the generic synthesis route described above.

Using viscosin and WLIP, two Viscosin (9:7) group members with known stereochemistry, we first establish that controlled hydrolysis of the depsi bond can be achieved. Next, we demonstrate that NMR-based fingerprinting continues to be an effective method for distinguishing diastereomers even when employing linear unstructured peptide analogues instead of the conformationally well-defined cyclic counterparts. Subsequently, we showcase the applicability and improved efficiency of our updated NMR matching approach by applying it to two different cases. First, we tackled putisolvin (12:4), a known but stereochemically undefined *Pseudomonas* CLiP, that resisted synthesis using our original total synthesis approach, and show that the originally proposed structure should be revised. Next, we introduce tanniamide, a CLiP newly isolated from *Pseudomonas ekonensis* COR58, a member of the Koreensis subgroup that harbors producers of Amphisin (11:9) and Bananamide (8:6) CLiPs. It defines a new group (12:10) with the largest macrocycle size reported to date within the *Pseudomonas* CLiP portfolio.

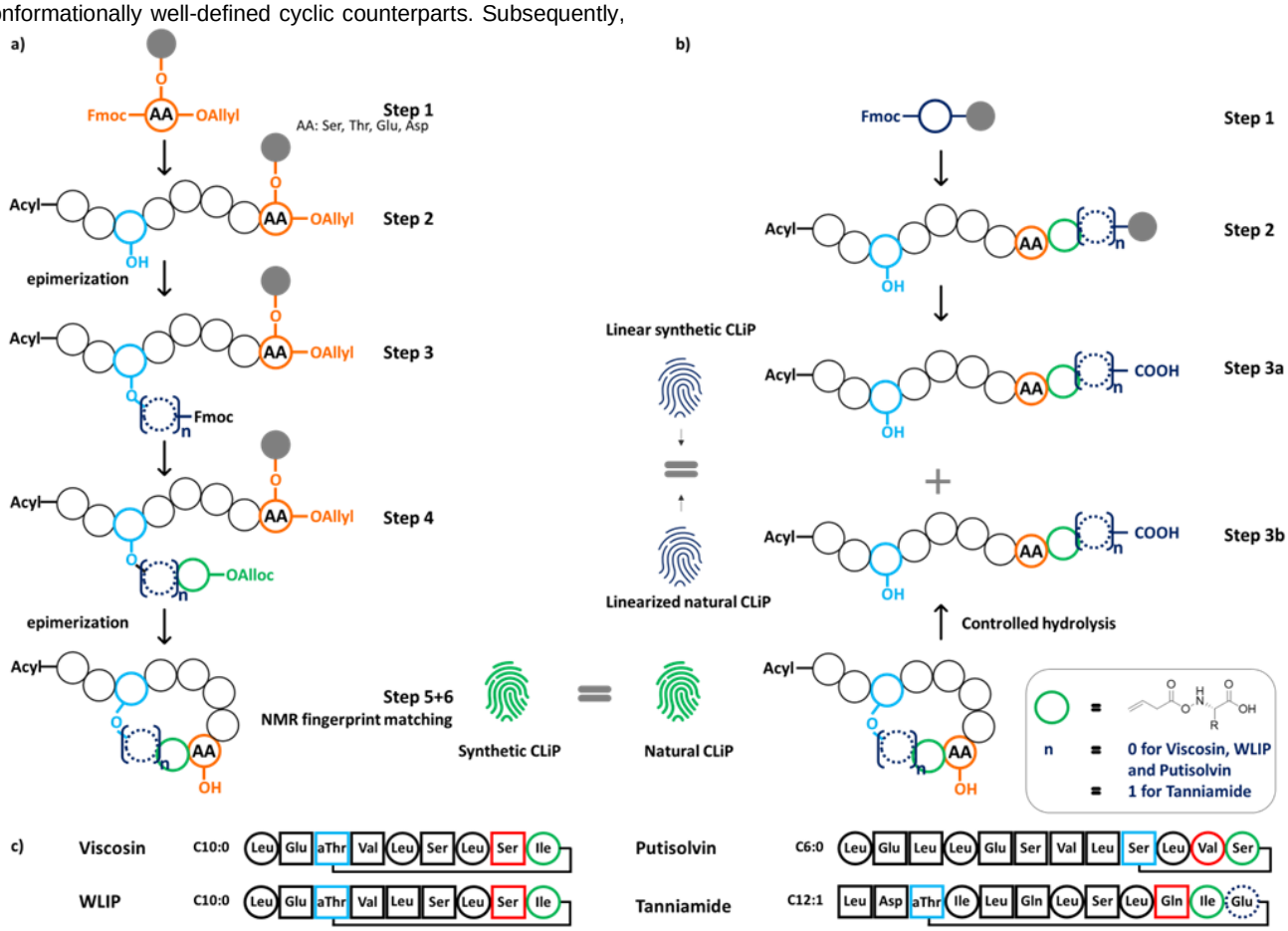

Scheme 1: Illustration of CLiP synthesis approaches for NMR fingerprinting purposes: (a) the conventional procedure, as reported by De Vleeschouwer *et al.* [7a], and (b) the saponification enhanced approach developed in this work. (c) displays the CLiP peptide sequences of interest in this work. In (a) and (b) circles denote individual amino acid residues with colors to indicate specific aspects of importance, differentiating both synthesis approaches. In (c) only, further differentiation is made by indicating D-amino acids using squares rather than circles, reserved for L-AA. In (a), orange denotes the starting amino acid required for anchoring on the 2-CTC resin which is preferably located close to the C-terminus (step 1). The synthesis proceeds through Fmoc/tBu SPPS (step 2). Light blue identifies the amino acid (Thr/Ser) with a free hydroxyl group involved in esterification (step 3). Dark blue indicates the future C-terminal residue(s) (n≥1) involved in esterification while the green residue in this segment represents the amino acid that will be involved in macrocycle closure. Here, the amino group is protected by Alloc, allowing orthogonal deprotection with the Allyl group of the resin anchored starting residue prior to lactamization and final release from resin (step 5) and fingerprinting against the natural compound. In some cases, the same amino acid residue is involved in the esterification and lactamization, (e.g. viscosin, WLIP and putisolvin). In (b) SPPS starts with resin anchoring of the C-terminal residue (step 1) followed by elongation up to the fatty acid chain (step 2) prior to release from the resin as a linear peptide (step3a). Color codes are maintained to facilitate comparison of amino acid residue positions relative to (a). Its NMR fingerprint is then compared against that of the linearized natural compound, obtained through controlled hydrolysis via saponification (step 3b).

Results and Discussion

Saponification-Enhanced NMR Fingerprint Matching: Proof of Principe using viscosin and WLIP.

We previously showed that CLiPs that only differ in the configuration of at least one amino acid give rise to NMR ^{1}H-{^{13}C} HSQC (CHα) fingerprints that are sufficiently distinct to allow their use for discrimination and dereplication purposes.[10a, 16] Given that the macrocycle imposes a specific CLiP conformation with associated characteristic chemical shift fingerprint, we first investigated to what extent its absence impacts the applicability of this fingerprint-based matching approach (objective 1), before devising conditions for controlled linearization by ester bond hydrolysis (objective 2).

We used two CLiPs with identical planar structure that belong to the Viscosin (9:7) group of *Pseudomonas* CLiPs. Each comprises nine amino acids, seven of which participate in the macrocycle through formation of an ester bond between the side chain alcohol moiety of the D-*allo*-Thr3 and the C-terminal carboxyl function. Both compounds adopt a clipped helix motif, consisting of a 6-residue α-helix at the N-terminus followed by a loop that clips the C-terminus onto the body of the α-helix.[16] This creates a rigid conformation that remains unaffected in a variety of environments.[17] Significantly, for our purposes, both compounds differ solely in the configuration of Leu5, with viscosin featuring L-Leu5 and WLIP featuring D-Leu5. The conformational impact of the D/ L-Leu5 switch remains limited to a rearrangement of the boundary between hydrophobic and hydrophilic surfaces yet provides a clearly distinct ^{1}H-{^{13}C} HSQC (CHα) fingerprint (Figure 1A). To assess the impact of linearization on fingerprint discrimination, linear analogues of viscosin and WLIP, as would be obtained from controlled hydrolysis of the native, cyclic compounds, were obtained using standard SPPS and purification. As is evident for both CLiPs, the respective fingerprint region, that features all (CHα) cross-peaks as well as (CHβ) cross-peaks associated with Ser/Thr, is considerably impacted by the loss of the macrocycle, and appears less well dispersed in the ^{1}H dimension, in agreement with the absence of the well-defined clipped helix conformation. (Figure 1B) The largest change is observed for the Thr3 (CHβ) methyn unit (^{1}H/^{13}C 5.41/69.5 ppm for viscosin and 5.47/69.4 for WLIP) which is strongly shifted to higher field (^{1}H/^{13}C 4.03/67.7 ppm, respectively, 4.10/67.7 ppm) in agreement with the lack of conversion of the secondary alcohol functionality into an ester bond. Despite the reduced dispersion, the fingerprint of linear viscosin remains sufficiently distinct from that of linear WLIP to allow clear discrimination. Therefore, we conclude that, even when differing solely in the configuration of a single amino acid, the NMR fingerprints of linear CLiP analogs retain sufficient uniqueness to serve as discriminators.

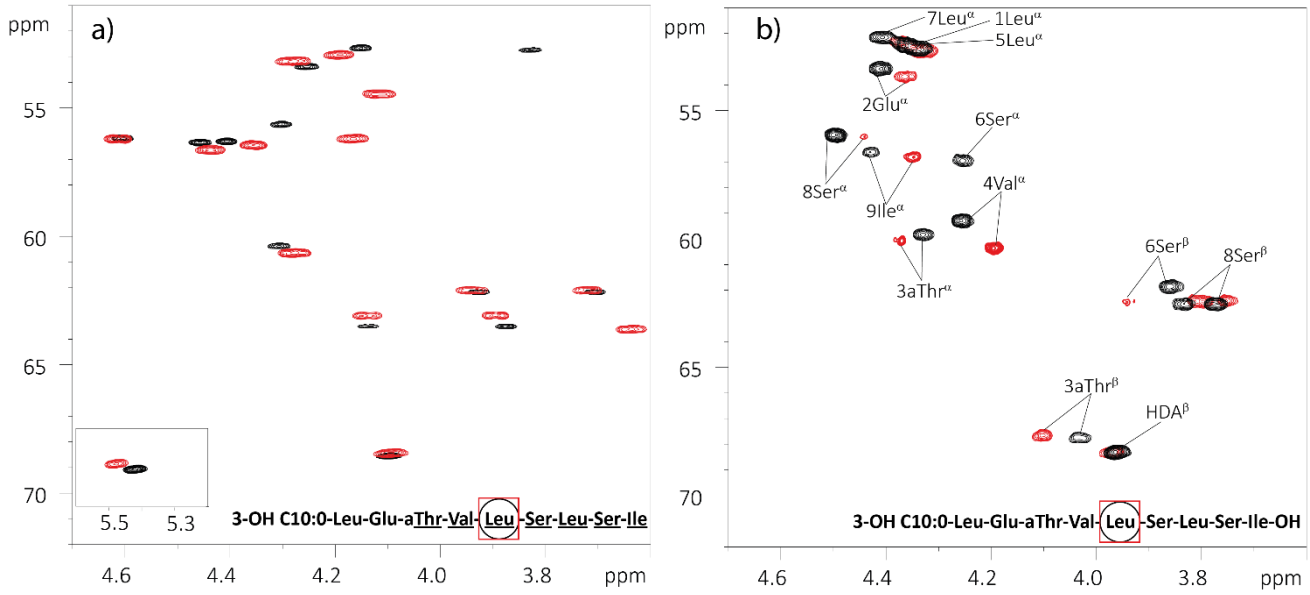

Figure 1: Comparison of the (CHα) NMR fingerprints of (a) cyclic and (b) linear viscosin (black) and WLIP (red). (700MHz, DMF-d7, 298K) The label HDA indicates 3-hydroxydecanoic acid.

With objective 1 achieved, we next moved to devise a protocol for linearization of CLiPs through controlled hydrolysis using viscosin as model for native CLiPs. First, the stability of the ester bond after 24h in basic conditions was investigated for buffered solutions at pH 8 and 10 and at pH 12, using HPLC (Supplementary Figures S1-S2). When dissolved in a phosphate buffer at pH 8, viscosin maintains stability over a 24h period since no degradation was apparent from the chromatogram. Incubating viscosin (**1**) in a carbonate-bicarbonate buffer at pH 10 initially suggests similar hydrolytic stability. However, after 24 hours, two products with significantly lower retention times (3.74 min (**2**) and 3.83 min (**3**) as compared to 4.90 min for **1**) suggesting a more polar character than original viscosin, were observed in the HPLC chromatogram. At pH 12, the hydrolysis process occurred much faster, with full conversion into the two products already observed after a 24-hour incubation period.

Mass analysis of the first eluting compound **2** shows it has a molecular mass (M) of 1143.5 Da (M(viscosin)+18 Da), while **3** eluting shortly thereafter is isobaric to viscosin (1125.5 Da). An 18 Da mass increase is expected upon hydrolysis of the viscosin ester bond through a nucleophilic acyl substitution mechanism involving OH^- as the incoming nucleophile (Scheme 2a), suggesting **2** corresponds to the desired linear variant of viscosin. This is further confirmed following complete NMR assignment. Notably, the Thr3 (CHβ) methyn unit, shows the expected upfield shifts caused by the release of the secondary alcohol from its ester. Gratifyingly, the retention time in HPLC and the NMR fingerprint of **2** is identical to that of the linear viscosin analogue obtained through SPPS (*vide supra*), unequivocally confirming its identity.

A competing mechanism that should be considered under basic conditions involves deprotonation at the alpha position of D-allo-Thr3, with formation of a double bond and concomitant elimination of the ester functionality resulting in macrocycle opening (Scheme 2b). The formation of this 2-amino-2-butenoic acid moiety (often referred to as Dhb in peptides issued from NRPS biosynthesis) results in a product that is isobaric with the parent compound.

In situ 1D ^{1}H NMR monitoring of the hydrolysis of viscosin in an acetonitrile:water solution at pH 12 indeed revealed the emergence of a quadruplet at 6.60 ppm, with 7.3 Hz scalar coupling. Position and multiplicity are consistent with the alkene proton of a 2-amino-2-butenoic acid moiety. By using a 1D selective ^{1}H TOCSY, scalar coupling to a methyl doublet appearing at 1.69 ppm could effectively be demonstrated, proving that **3** occurs from linearization by base catalyzed *E2* elimination. (Supplementary Figure S3) The ester bond stability in viscosin was also examined in acidic conditions using solutions at pH 5, 3, 2 or 1. Incubating the compound at pH 5 and 3, appears to have no effect and viscosin remains stable even after three days (*data not shown*). Incubation of viscosin at pH 1 or 2 does cause a marked decrease of the viscosin signal in the HPLC chromatogram without appearance of new contributions, likely indicating the total hydrolysis of viscosin at low pH. (Supplementary Figure S4). Given controlled hydrolysis through saponification was already achieved under basic conditions, acidic conditions were not investigated any further.

With the successful achievement of our initial objectives, we advanced to apply and further validate the method by determining the configuration of putisolvin and tanniamide using saponification enhanced NMR fingerprinting.

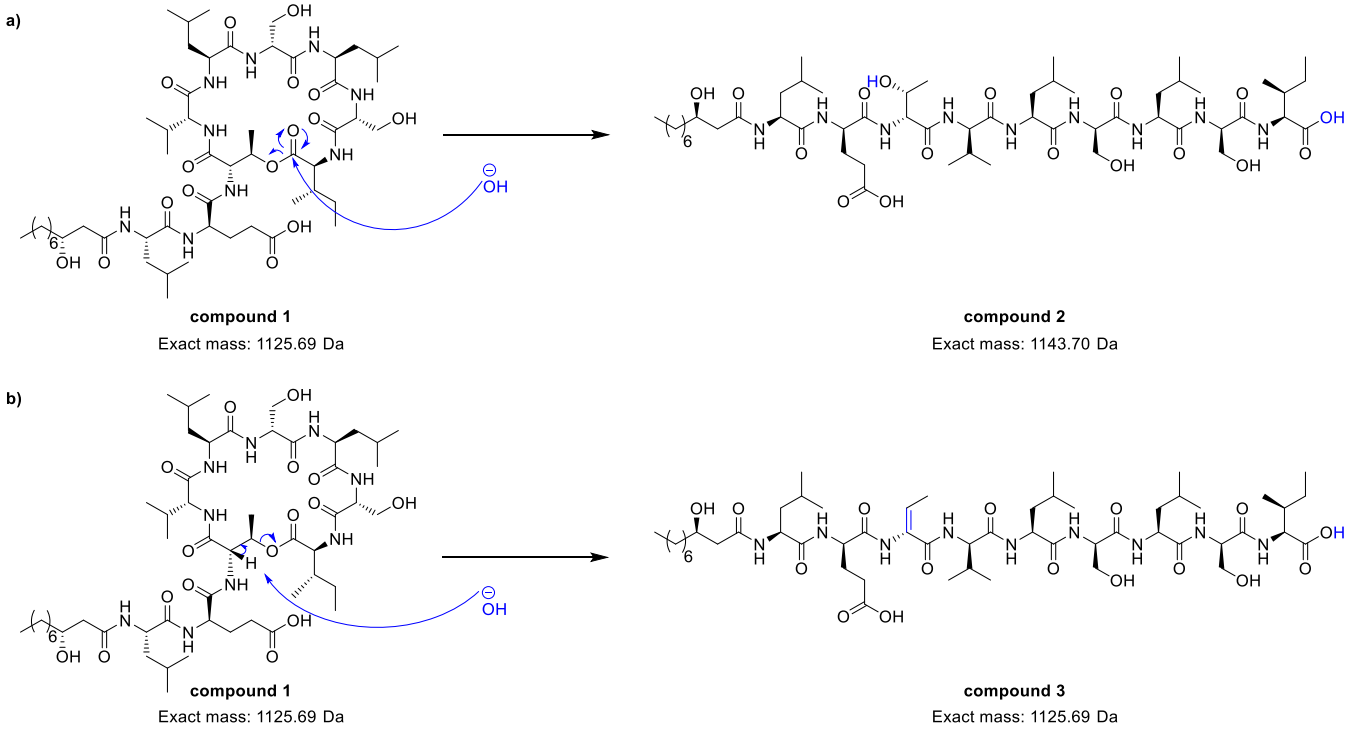

Scheme 2: Possible reaction mechanisms for the basic hydrolysis of viscosin.

Structural Characterization of Putisolvin

Putisolvin as used in this work was extracted from its original producer, *Pseudomonas putida* PCL1445, which was isolated from soil heavily polluted with polyaromatic hydrocarbons.[18] For the extraction of the CLiPs, we utilized the original methodologies and subsequently purified them via reverse-phase HPLC (Supplementary Figure S5). In addition to the major fraction, a single minor fraction was also collected, and both underwent *de novo* structure analysis using a combination of NMR spectroscopy and mass spectrometry to establish their planar structure.

The major CLiP (**4**), eluting at 11.2 minutes, consists of a fatty acid connected to a peptide chain comprising 12 amino acids (5x Leu, 3x Ser, 2x Val, 1x Glu, 1x Gln) (Supplementary Figure S6, Supplementary Tabel S1). Following amino acid residue type annotation using 2D TOCSY, the sequence as shown in Table 1 was firmly established via 2D ROESY and ^{1}H–{^{13}C} gHMBC spectra. Furthermore, the previously suggested participation of Ser9 and Ser12 in ester bond formation is now definitively confirmed by a distinct $^3J_{CH}$ cross-peak connecting Ser9 Hβ1,2 and Ser12 C' in the ^{1}H–{^{13}C} gHMBC spectrum. This observation

also aligns with the substantial downfield shift of both Ser9 Cβ and Hβ1,2 resonances. Thus, the AA sequence of the major putisolvin is Leu1-Glu2-Leu3-Leu4-Gln5-Ser6-Val7-Leu8-Ser9-Leu10-Val11-Ser12. Confrontation with mass spectrometric data allows confirmation of an N-capping hexanoic fatty acid moiety (C6:0). The fatty acid chain thus lacks the 3-hydroxyl functionality typical for most *Pseudomonas* CLiPs. The minor compound (**5**), eluting at a retention time of 15.6 minutes, was identified as a homologue of the main compound, with a mass lower by 14 Da. NMR analysis showed it features an Ile11 as opposed to Val11 in the main compound (Supplementary Table S2). Such Ile/Val homologues are a typical outcome of A-domain substrate flexibility.[19]

As both putisolvins were isolated from the same bacterial strain, the major and minor compounds isolated here were expected to respectively correspond to putisolvin I and II as characterized by Kuiper et al.[18] However, our sequences deviate from those of putisolvin I and II as we established Leu4/Leu8 residues instead of Ile4/Ile8. It is noteworthy that these represent isobaric substitutions that do not raise conflict with the previously reported mass spectrometric data analysis that was used as the main source for structure elucidation. Although NMR spectral data was involved, none was published by Kuiper et al[18], preventing the use of our NMR based fingerprinting method to assess whether a revision of the chemical structures is in order.

However, the sequences isolated in this work are identical to those for putisolvin III and IV previously isolated from *Pseudomonas sp.* COR19[20] and for which NMR spectral data is available from the rhizoclip website (www.rhizoclip.be). Comparison of the respective ^{1}H-{^{13}C} HSQC of putisolvin III and IV to respectively the major and minor putisolvin from *P. putida* PCL 1445 reveals a perfect match (Supplementary Figure S7), proving structural identity including stereochemistry, even though the latter remains to be explicitly established (vide infra). Since we established that sequences for putisolvin III are also produced as major compound in *Pseudomonas* sp. COR55, *Pseudomonas* sp. NNC7, *Pseudomonas vlassakiae* WCU_60/WCU_64, *Pseudomonas capeferrum* WCS358^{T} and *Pseudomonas fulva* LMG 11722^{T}, (Supplementary Figures S8-S12) and the biosynthetic gene clusters (BGCs) of these demonstrate high levels of genetic similarity[1a], we propose the sequences for putisolvin I and II should be revised.

Given that the stereochemistry of putisolvin I was previously only available as a prediction from bioinformatic analysis of the *P. putida* PCL1445 BGC [21], our first objective was to confront this with Marfey's analysis. Applied to putisolvin I this revealed the presence of 2x D-Ser, 1x L-Ser, 2x D-Glx, 3x L-Leu, 2x D-Leu, 1x D-Val, 1x L-Val. Consequently, there is configurational heterogeneity for Ser, Val and Leu and positional information on the distribution of D- and L-configured residues is lost. Collectively, a total of 60 possible diastereomeric sequences should therefore be considered. This can be reduced to more manageable proportions by establishing the nature of the condensation domains in the NRPS assembly line. Present in each NRPS module, these domains extend the growing peptide chain by an additional amino acid. In case of dual function E/C domains, the residue at the preceding position is in principle epimerized from L to D, whereas $^{L}C_{L}$ condensation domains lack epimerization activity and leave the configuration unchanged. Because of the latter, the presence of and $^{L}C_{L}$ domain can be used to pinpoint L-configured resides in the NRPS product with certainty. In contrast, not all E/C domains effectively perform the L to D epimerization thus leaving ambiguity in establishing the actual configuration.[11, 22] Analysis of the NRPS system of *P. putida* PCL1445 with AntiSMASH shows $^{L}C_{L}$ domains are present in module 11 and 12, in agreement with the previous findings by Dubern et al. [21]. This allows to fix the stereochemistry of the terminal tripeptide to L-Leu– L-Val– L-Ser, the latter residue being L-configured by default as there is no subsequent module in the NRPS assembly line. Using the outcome of Marfey's analyses (vide supra), this automatically fixes the configuration of Ser6, Val7 and Ser9 to D- and reduces positional ambiguity to that of 2 L-Leu and D-Leu residues only. In all, analysis of the condensation domains allows to bring down the number of possible diastereoisomeric sequences from 60 to 6 as summarized in putisolvin (12:4)-Lx sequences. (Table 1)

Based on the above, we originally considered embarking on total chemical synthesis of the six consensus cyclic sequences to establish the stereochemistry of putisolvin I. However, though putisolvin features three serine residues, none of these are suitable as a starting point for resin anchoring and further synthesis. As the residue provides the alcohol for ester bond formation, Ser9 cannot be side chain anchored. Since Ser6 is located in the exocyclic part of the peptide, anchoring here followed by peptide extension to the N-terminus with Fmoc-based SPPS does not allow to build the macrocycle. The remaining Ser12 residue is, at the same time, the C-terminal residue, as well as the one involved in ester bond formation (with Ser9) rendering it undesirable as side chain-anchored starting point of the synthesis. Effectively, on resin macrolactonisation (rather than macrolactamisation) is then needed and would involve formation of a strained 4-amino acid residue ring, which is expected to be particularly challenging by the high sterical hindrance resulting from the side chain immobilization of the Ser12 residue. These significant challenges underscore the constraints of our current synthesis approach and prompted the development of the saponification enhanced approach, which was first validated as described above.

Table 1: Sequence, configurational analysis, and stereochemical assignment of putisolvin from P. putida PCL1445.

P. putida PCL1445	AA1	AA2	AA3	AA4	AA5	AA6	AA7	AA8	AA9	AA10	AA11	AA12
Bioinformatic analysis pathway												
A domain	Leu	Glu	Leu	Leu	Gln	Ser	Val	Leu	Ser	Leu	Val	Ser
C domain	C1	E/C	E/C	E/C	E/C	E/C	E/C	E/C	E/C	E/C	$^{L}C_{L}$	$^{L}C_{L}$
Prediction	D	D	D	D	D	D	D	D	D	L	L	L
Chemical analysis pathway												
NMR analysis	Leu	Glu	Leu	Leu	Gln	Ser	Val	Leu	Ser	Leu	Val	Ser
Marfey's analysis	L/D	D	L/D	L/D	D	L/D	L/D	L/D	L/D	L/D	L/D	L/D
Combined analysis and synthesized (12:4) diastereomeric sequences												
	Leu	Glu	Leu	Leu	Gln	Ser	Val	Leu	Ser	Leu	Val	Ser
(12:4) D1D3 (6)	D	D	D	L	D	D	D	L	D	**L**	**L**	**L**
(12:4) D3D4 (7)	L	D	D	D	D	D	D	L	D	**L**	**L**	**L**
(12:4) D4D8 (8)	L	D	L	D	D	D	D	D	D	**L**	**L**	**L**
(12:4) D3D8 (9)	L	D	D	L	D	D	D	D	D	**L**	**L**	**L**
(12:4) D1D8 (10)	D	D	L	L	D	D	D	D	D	**L**	**L**	**L**
(12:4) D1D4 (11)	D	D	L	D	D	D	D	L	D	**L**	**L**	**L**

* The nomenclature of the synthetic compounds is based on the (l:m) notation of the Putisolvin group (12:4), where the length 'l' represents the total number of amino acids while 'm' indicates those involved in the macrocycle. The (l:m) notation is followed by the configuration and position of the 2 D-leucines in the putisolvin I sequence (positions 1, 3, 4 or 8), implicitly placing the two L-Leucines in the other positions. Red font is used to indicate ambiguous configuration. Underlined residues are part of the confirmed macrocycle.

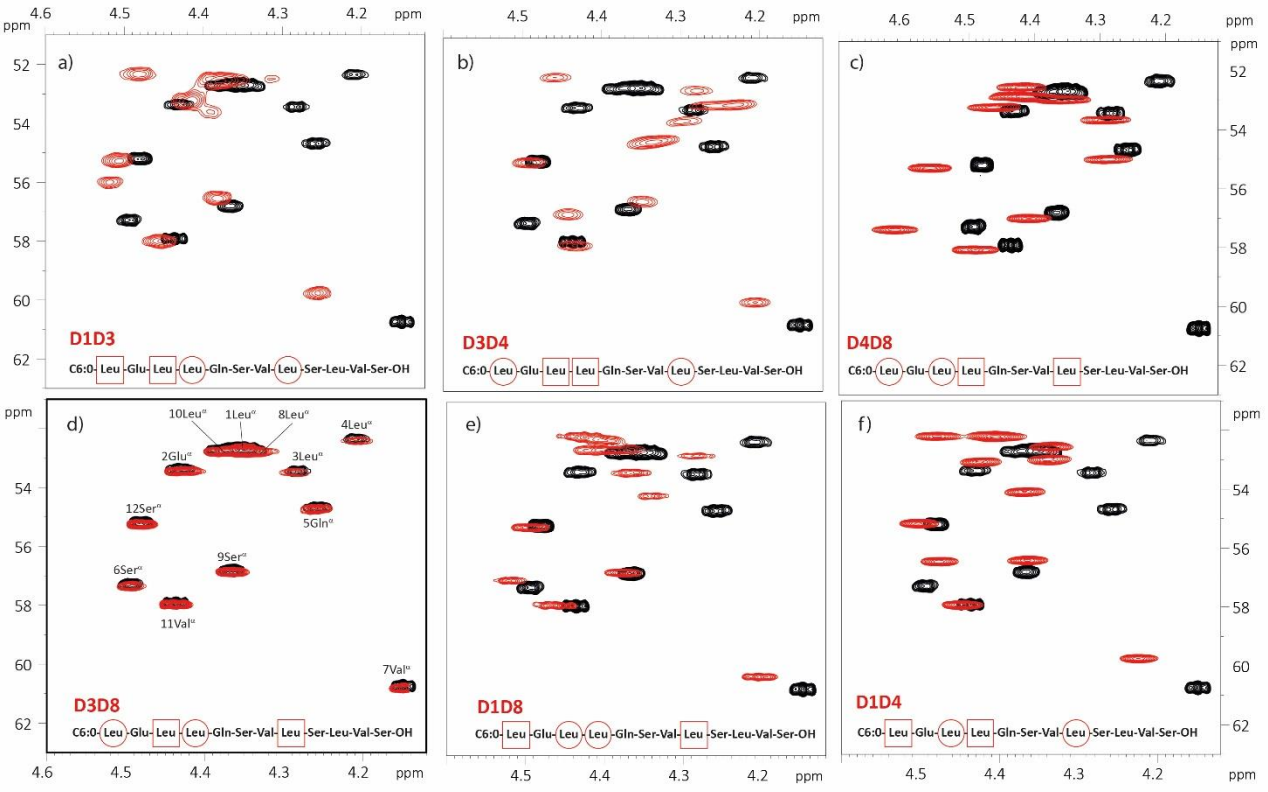

Figure 2: Comparison of the ^{1}H-{^{13}C} HSQC (CHα) fingerprints of the various synthetic (12:4)-DxDx variants (red) with that of the linear putisolvin (black) recorded in DMF-d7 at 700 MHz, 298K. a) D1D3 (**6**), b) D3D4 (**7**), c) D4D8 (**8**), d) D3D8 (**9**), e) D1D8 (**10**), f) D1D4 (**11**)

Natural, purified putisolvin I (**4**) was exposed to basic conditions (pH=10 (NaOH)) and monitored by RP-HPLC. Complete hydrolysis of the depsi bond was achieved at room temperature within 4h. A single product emerged with a mass corresponding to the desired hydrolyzed product, as confirmed by MS (+18 Da, Supplementary Figures S13-S14). Complete NMR assignment reveals the expected upfield shift of the Ser9 CH_2^{β} ^{1}H and ^{13}C resonances upon release of the secondary alcohol from the ester. (Supplementary Figures S15). For putisolvin, no elimination product is generated, leading to a more favorable saponification outcome compared to viscosin. Since the occurrence of (complete) epimerization at a particular Ca during saponification cannot entirely be excluded, the procedure was repeated using a solution of sodium deuteroxide in D_2O (4h, rt). Epimerization under these conditions should introduce a deuterium in the backbone, reducing or removing the corresponding Hα resonance in the ^{1}H NMR spectrum and (CHα) correlation in the ^{1}H-{^{13}C} HSQC. Since no such effects could be detected epimerization during saponification could confidently be excluded (Supplementary Figure S16-S17).

With linearized putisolvin (**12**) in hand, we proceed to compare its (CHα) fingerprint with that of the 6 synthesized linear diastereoisomers (Table 1, Supplementary Figures S20-S26, Supplementary Tables S3-S8). A straightforward visual assessment of the respective overlays in Figure 2 clearly indicates that the (12:4)D3D8 (**9**) variant displays a quasi-perfect fingerprint match with linearized putisolvin (**12**) (Figure 2d) while considerable to almost complete mismatches exist with those of the other synthetic homologues. A more quantitative assessment based on combined chemical shift (dis)similarity is provided in Supplementary Figures S18-S19. The stereochemistry of native putisolvin I (**4**) corresponds to that of the (12:4)-D3D8 (**9**) synthetic sequence (C6:0 – L-Leu – D-Glu – D-Leu – L-Leu – D-Gln – D-Ser – D-Val – D-Leu – D-Ser – L-Leu – L-Val – L-Ser, whereby the underlined amino acids indicate those that are part of the macrocycle). Since Leu1 and Leu4 are L-configured, it can be concluded that the E/C domains of module 2 and 5 in the putisolvin-producing NRPS are epimerisation-inactive.

Structural Characterization of Tanniamide

To showcase the generic potential of linearization through controlled hydrolysis by saponification prior to NMR fingerprint matching as a means to elucidate CLiP stereochemistry, we proceeded to apply this to tanniamide, a newly isolated CLiP giving rise to a new group in the *Pseudomonas* CLiPs.

Tanniamides were extracted from a bacterial culture of *P.* ekonensis. COR58 in KB medium, using previously described protocols. [20, 23] This bacterium was initially isolated from the rhizosphere of red cocoyam in Cameroon. [23] The name of the CLiP (previously identified as N4 [10,12]) refers to 'tannia', the common local term for cocoyam, a staple crop in Cameroon. Following bacterial growth, the crude extract was subjected to reverse phase HPLC purification, and three fractions were collected and fully characterized. (Supplementary Figure S27-S28, Supplementary Tables S9-11)

Mass spectrometry showed that the major compound, tanniamide A (**13**), has a molecular mass of 1563.75 Da, placing it in a mass range previously not observed for *Pseudomonas* CLiPs. (Supplementary Figure S29). NMR spectroscopic analysis of 2D ^{1}H-^{1}H TOCSY and ROESY spectra in DMF-d7 revealed 4x Leu, 2x Ile, 2x Gln, 1x Glu, 1x Thr, 1x Ser and 1x Asp. Next, their distribution over the oligopeptide sequence was established by observing sequential H^{N}-H^{N} and H^{α}-H^{N} cross-peaks in the 2D ^{1}H-^{1}H ROESY spectrum, revealing the planar sequence as shown in Table 2. The presence of 3-hydroxydodec-5-enoic acid (C12:1) was determined by a combined analysis of NMR and mass spectrometric data. Using the same reasoning as applied for xantholysin, the ^{13}C chemical shifts of the alkene function indicate a cis (Z) configuration. [24] The proposed involvement of Thr3 in the depsi bond was confirmed by analyzing the ^{1}H-^{13}C gHMBC spectrum, which showed a clear cross-peak between Thr3 CH^{β} and Glu12 C', while characteristic upfield ^{1}H and ^{13}C chemical shifts could be observed for Thr3 CH^{β}.

Tanniamides B (**14**) and C (**15**) could also be purified and characterized as minor compounds. Featuring a mass of 1563.92 Da (isobaric) and 1565.94 Da (+2 Da), NMR analysis allowed to identify these minors as tanniamide A homologues, featuring Ile 11 in place of Leu 11 and a saturated C12:0 acyl chain respectively. These three compounds represent new CLiPs that cannot be placed in any of the existing *Pseudomonas* CLiP groups as defined by their (l:m) tag. Therefore, they make up a novel *Pseudomonas* group that we will denote as the Tanniamide (12:10) group. To map the presence of epi-inactive domains and pave the way to its 3D structure determination, we engaged into establishing the stereochemistry of tanniamide, starting with Marfey's analysis. Despite extensive optimization of chromatographic conditions (Supplementary Material), the configuration of only nine amino acids could be confidently identified: 2x L-Leu, 1x D-Leu, 2x D-Glx, 1x D-Ser, 1x D-aThr, 1x D-Asp and 1x L-Ile, the remaining Leu, Ile and Glx residues appearing absent most likely due to incomplete hydrolysis of the C-terminus (Supplementary Figures S37-S38).

With the genomic sequence of *P. ekonensis* COR58 being available, A-domain analysis of the COR58 BGC enabled prediction of a dodecapeptide sequence from the associated NRPS, in line with our NMR analysis (

). Next, the nature of the condensation domains was evaluated to assess whether they belong to the $^{L}C_{L}$ or E/C subdomain. The initial C^{start} domain responsible for the incorporation of the fatty acid is followed by six dual activity E/C domains. This is followed by an alternating pattern of $^{L}C_{L}$ and E/C type domains, ending with an $^{L}C_{L}$ domain in module 12 (Table 2). Considering the location of the $^{L}C_{L}$ domains, Leu7, Leu9 and Ile11 must be L-configured, as is the C-terminal L-Glu12 by default. Combining this with the results from Marfey's allows to deduce a limited number of diastereomeric sequences for NMR fingerprint matching. First, the identification of Gln residues at position 6 and 10 by NMR, the L-configuration of Glu12, and the identification of 2 D-GLx residues from Marfey's, implies both Gln to be D-configured. Next, the 1:2 D:L ratio for leucines together with the presence of L-Leu7 and L-Leu9 implies the presence of at least one D-Leu at either position 1 or 5; the configuration of the last Leu remains unclear as this point. Thus, D1D5, D1L5 or L1D5 but no L1L5 combinations should be considered, with either L containing combination requiring an epimerization inactive E/C domain in module 2 respectively 6 of the NRPS. Finally, with one L-Ile identified from Marfey's analysis and the assumed presence of L-Ile11, it remains to be established whether Ile4 is L- or D-(allo) configured. This doubles the number of diastereomeric homologues to be evaluated with NMR fingerprint matching from 3 to 6. (Table 2).

Similar to putisolvin I, an aqueous NaOH solution, pH 11 was used for controlled hydrolysis through saponification (Supplementary Figure S30). For tanniamide, complete hydrolysis required a 4-to-5-day reaction time at 40°C, indicating much slower reaction kinetics compared to viscosin and putisolvin I. The reaction was performed in parallel with NaOD in D_2O to check for epimerization. In both cases, HPLC indicated the formation of a single reaction product (**16**), with a mass reflecting the expected increase of 18 Da (20 Da in deuterated conditions) (Supplementary Figures S31-S32). Hydrolysis of the ester bond was further confirmed by full NMR characterization (Supplementary Figures S33-S36). As with putisolvin I, the Thr3 (CHβ) ^{1}H and ^{13}C resonances shift upfield due to the release of the secondary alcohol from the ester. Importantly, no (CHα) resonances are missing or affected in intensity in the ^{1}H-^{13}C HSQC spectrum of tanniamide linearized under deuterated conditions, proving the absence of epimerization during saponification.

Table 2: Sequence, configurational analysis, and stereochemical assignment of tanniamide A from P. ekonensis COR58

P. ekonensis COR58	AA1	AA2	AA3	AA4	AA5	AA6	AA7	AA8	AA9	AA10	AA11	AA12
Bioinformation analysis pathway												
A domain	Leu	Asp	Thr	Ile	Leu	Gln	Leu	Ser	Leu	Gln	Ile	Glu
C domain	C1	E/C	E/C	E/C	E/C	E/C	E/C	$^{L}C_{L}$	E/C	$^{L}C_{L}$	E/C	$^{L}C_{L}$
Prediction	D	D	D	D	D	D	L	D	L	D	L	L
Chemical analysis pathway												
NMR analysis	Leu	Asp	Thr	Ile	Leu	Gln	Leu	Ser	Leu	Gln	Ile	Glu
Marfey's analysis	L/D	D	D	L	L/D	L/D	L/D	D	L/D	L/D	L/D	L/D
Combined analysis and synthesized (12:10) diastereomeric sequences												
	Leu	Asp	Thr	Ile(*)	Leu	Gln	Leu	Ser	Leu	Gln	Ile	Glu
(12:10) D1L4D5 (17)	D	D	D	L	D	D	L	D	L	D	L	L
(12:10) L1L4D5 (18)	L	D	D	L	D	D	L	D	L	D	L	L
(12:10) D1L4L5 (19)	D	D	D	L	L	D	L	D	L	D	L	L
(12:10) D1D4D5 (20)	D	D	D	D	D	D	L	D	L	D	L	L
(12:10) L1D4D5 (21)	L	D	D	D	D	D	L	D	L	D	L	L
(12:10) D1D4L5 (22)	D	D	D	D	L	D	L	D	L	D	L	L

* The nomenclature of the synthetic compounds is based on the (l:m) notation of the N4 group (12:10), where the length 'l' represents the total number of amino acids while 'm' indicates those involved in the macrocycle. The (l:m) notation is followed by the configuration and position of the Leu1, Ile4 and Leu5 respectively. . Red font is used to indicate ambiguous configuration. (*¨) when D-configured, the *allo*-stereoisomer is included. The underlined amino acids indicate those that are part of the macrocycle

Synthesis of the linear diastereoisomers proposed in Table 2 was performed using standard Fmoc-based SPPS (Supplementary Figures S39-S45). For practical convenience, a (3*R*)-hydroxydecanoic acid moiety was used for N-capping, instead of the (R,Z)-3-hydroxydodec-5-enoic acid. This substitution is viable since in our experience variations in the fatty acid tail do not affect the chemical shifts of the peptide backbone. [10a] All thus obtained synthesized linear analogues of tanniamide were fully characterized by NMR. (Supplementary Tables S13-S19) As observed before, the different configurations yield prominent differences in α-CH region of ^{1}H-{^{13}C} HSQC spectrum. (Figure 3) The overlay of the respective fingerprints with that of the linearized natural tanniamide provides a straightforward visual identification of the matching configuration: the (12:4) D1D4L5 (**22**) diasteromer displays a quasi-perfect fingerprint match with linearized tanniamide (**16**) (Figure 3Figure 3f) while considerable mismatches exist with those of the other synthetic homologues. (Supplementary Figure S46) The match extends to the 3-hydroxy group, which was introduced as 3R in all linear diastereomers, based upon the nearly isochronous ^{1}H resonances of the preceding CH_2 moiety, as opposed to clearly separated resonances for the 3S configuration.[10a]

All data together establish that the stereochemistry of cyclic tanniamide A corresponds to that of the linear (12:10) D1D4L5

(**22**) synthetic analogue. The structure of tanniamide A (**13**) is therefore (R,Z)-3-hydroxydodec-5-enoic acid - D-Leu – D-Asp – D-aThr – D-aIle – L-Leu – D-Gln – L-Leu – D-Ser – L-Leu – D-Gln – L-Ile – L-Glu. Since Leu5 is L-configured, it can be concluded that the E/C domain of module 6 in the tanniamide-producing NRPS is epimerisation-inactive.

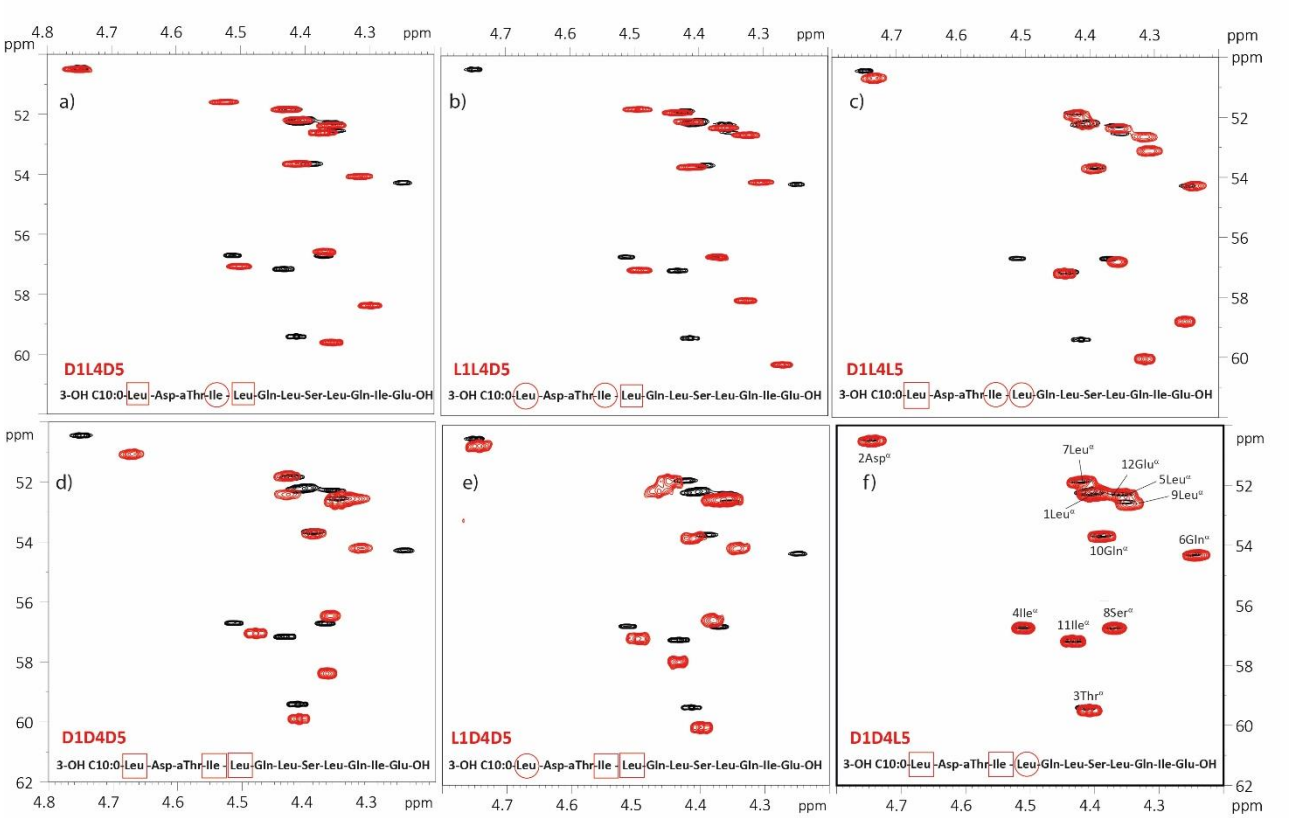

Figure 3: Comparison of the ^{1}H-{^{13}C} HSQC (CHα) fingerprints of the various synthetic (12:10) variants (red) with that of the linear tanniamide (black) recorded in DMF-d7 at 700 MHz, 298K

Conclusion

CLiPs constitute a class of bioactive compounds with clear application potential. Determining their stereochemistry is therefore essential to establish structure-activity relationships and for determining their 3D structure as means to understand and modulate their properties. Unfortunately, conventional chemical methods such as Marfey's analysis are not consistently straightforward in their outcome while bioinformatic analysis of the NRPS BGC is unable to predict with high confidence if epimerization domains are fully functional. Our previously described NMR fingerprint matching approach provides a fast and reliable tool for the dereplication of newly isolated CLiPs, whereby the NMR fingerprint of a newly isolated CLiP is compared to that of a reference with known stereochemistry, available from a publicly available database (https://www.rhizoclip.be).[10a] In absence of a match, we showed that chemical synthesis of a small library of 'consensus' sequences issued from all available data may be used to tackle stereochemical dead-ends, and has led to the structural elucidation of CLiPs in the Bananamide (8:6), Orfamide (10:8), Xantholysin (14:8) and Entolysin (14:5) groups.[10a, 11] The synthetic burden accompanying the introduction of the macrocycle, even requiring a complete redesign of the synthesis strategy, motivated the development of a lean and more generally applicable approach for depsipeptide macrocycles. More specifically, we established that our NMR fingerprinting approach still works when using the (CHα) fingerprint of linear diastereomeric sequences, obtained through classic SPPS, against the fingerprint of the linearized version of the natural compound, itself obtained through controlled saponification of the depsi bond. Even when differing solely in the configuration of a single amino acid, the NMR fingerprints of linear CLiP analogs retains sufficient uniqueness to serve as discriminators.

Its application to the structural characterization of putisolvin from *P. putida* PCL1445 revealed discrepancies in the originally published sequences. Our analysis rectified these errors, establishing putisolvin III and IV to be identical to putisolvin I and II, whose characterization needed to be revised. This enabled the subsequent use of NMR fingerprint matching as a dereplication tool for CLiPs produced by several *Pseudomonas* species of the Putida group, that are all shown to produce putisolvin I as major CLiP.

A further demonstration of the broad applicability of our saponification enhanced fingerprint approach involved the full characterization of tanniamide A, a novel CLiP from *P. ekonensis*. COR58 defining a novel (12:10) group in the *Pseudomonas* CLiP portfolio. While having the same number of amino acids in its sequence as putisolvin, the macrocycle encompasses 10 amino acids rather than 4, representing the largest macrocycle reported to date for the more than 130 reported *Pseudomonas* CLiPs. Several *Pseudomonas* strains isolated from sugarcane-cultivated soils in Brazil[25] carry a BGC that is highly similar to the COR58 NRPS gene cluster, likely encoding tanniamide production.[1a]

The NMR reference spectra of the cyclic CLiPs in this study have been incorporated into the Rhizoclip database. The results obtained for putisolvin and tanniamide also allowed to pinpoint specific NRPS modules with epi-inactive E/C domains, providing input for future efforts aiming at improved prediction of epimerization domain functionality. Given the ease of SPPS of linear peptide sequences and provided the depsi bond can be hydrolyzed in a controlled fashion, as demonstrated here for CLiPs from three different macrocycle sizes, our approach should find wide-spread application for the stereochemical elucidation of non-ribosomally synthesized lipodepsipeptides from a variety of sources.

Supporting Information

The authors have cited additional references within the Supporting Information.

Acknowledgements

A.M., M.H. and J.M. are recipients of a concerted research action grant (MEMCLiP) from Ghent University supporting this research (GOA-028-19). J.M., R.D.M., and M.H. are recipients of the Excellence of Science grant RhizoCLiP (EOS ID 30650620) supporting this research. The NMR equipment used in this work is part of the NMR Centre of Expertise, a UGent Core Facility, and was funded through the FFEU-ZWAP initiative and grants from the Hercules Foundation (AUGE09/06 and AUGE15/12) awarded to consortia headed by J. Martins. We thank Ilse Delaere for practical assistance with bacterial cultures, HPLC purifications, and NMR characterization.

Keywords: NMR spectroscopy, cyclic lipodepsipeptides, Pseudomonas, stereochemistry, dereplication, SPPS

References

[1] aC. Cesa-Luna, N. Geudens, L. Girard, V. De Roo, H. R. Maklad, J. C. Martins, M. Höfte, R. De Mot, *mSystems* **2023**, e00988-00922; bS. Andrić, T. Meyer, A. Rigolet, C. Prigent-Combaret, M. Höfte, G. Balleux, S. Steels, G. Hoff, R. De Mot, A. McCann, E. De Pauw, A. Argüelles Arias, M. Ongena, *Microbiol Spectr* **2021**, *9*, e0203821; cM. Rodríguez-Cisneros, L. M. Morales-Ruíz, A. Salazar-Gómez, F. U. Rojas-Rojas, P. Estrada-de los Santos, *Molecules* **2023**, *28*, 1646.

[2] T. Clements-Decker, M. Kode, S. Khan, W. Khan, *Frontiers in Chemistry* **2022**, *10*.

[3] aJ. D'Aes, N. P. Kieu, V. Leclere, C. Tokarski, F. E. Olorunleke, K. De Maeyer, P. Jacques, M. Höfte, M. Ongena, *Environ. Microbiol.* **2014**, *16*, 2282-2300; bJ. M. Raaijmakers, I. De Bruijn, O. Nybroe, M. Ongena, *FEMS Microbiol. Rev.* **2010**, *34*, 1037-1062.

[4] aJ. Prsic, M. Ongena, *Front. Plant. Sci.* **2020**, *11*, 594530; bS. Zhang, R. Mukherji, S. Chowdhury, L. Reimer, P. Stallforth, *Proc Natl Acad Sci U S A* **2021**, *118*; cS. Pflanze, R. Mukherji, A. Ibrahim, M. Günther, S. Götze, S. Chowdhury, L. Reimer, L. Regestein, P. Stallforth, *Chem. Sci.* **2023**, *14*, 11573-11581; dY. Hou, Y. Bando, D. Carrasco Flores, V. Hotter, R. Das, B. Schiweck, T. Melzer, H.-D. Arndt, M. Mittag, *New Phytol.* **2023**, *237*, 1620-1635.

[5] N. Geudens, J. C. Martins, *Front. Microbiol.* **2018**, *9*.

[6] M. Höfte, in *Microbial bioprotectants for plant disease management* (Eds.: J. Köhl, W. J. Ravensberg), Burleigh Dodds, **2021**, pp. 301-374.

[7] aM. De Vleeschouwer, D. Sinnaeve, J. Van den Begin, T. Coenye, J. C. Martins, A. Madder, *Chem. Eur. J.* **2014**, *20*, 7766-7775; bM. De Vleeschouwer, T. Van Kersavond, Y. Verleysen, D. Sinnaeve, T. Coenye, J. C. Martins, A. Madder, *Front. Microbiol.* **2020**, *11*.

[8] S. Gotze, P. Stallforth, *Nat. Prod. Rep.* **2020**, *37*, 29-54.

[9] S. Gotze, P. Stallforth, *Org. Biomol. Chem.* **2020**, *18*, 1710-1727.

[10] aV. De Roo, Y. Verleysen, B. Kovács, M. De Vleeschouwer, P. Muangkaew, L. Girard, M. Höfte, R. De Mot, A. Madder, N. Geudens, J. C. Martins, *Microbiology Spectrum* **2022**, *10*, e01261-01222; bK. Scherlach, G. Lackner, K. Graupner, S. Pidot, T. Bretschneider, C. Hertweck, *ChemBioChem* **2013**, *14*, 2439-2443.

[11] P. Muangkaew, V. De Roo, L. Zhou, L. Girard, C. Cesa-Luna, M. Höfte, R. De Mot, A. Madder, N. Geudens, J. C. Martins, *Int. J. Mol. Sci.* **2023**, *24*, 14302.

[12] aJ. Steigenberger, Y. Verleysen, N. Geudens, A. Madder, J. C. Martins, H. Heerklotz, *Biophys. J.* **2022**; bJ. Steigenberger, Y. Verleysen, N. Geudens, J. C. Martins, H. Heerklotz, *Front. Microbiol.* **2021**, *12*.

[13] Y. Bando, Y. Hou, L. Seyfarth, J. Probst, S. Götze, M. Bogacz, U. A. Hellmich, P. Stallforth, M. Mittag, H.-D. Arndt, *Chemistry – A European Journal* **2022**, *28*, e202104417.

[14] H. Y. Lam, Y. Zhang, H. Liu, J. Xu, C. T. Wong, C. Xu, X. Li, *J Am Chem Soc* **2013**, *135*, 6272-6279.

[15] M. De Vleeschouwer, J. C. Martins, A. Madder, *J. Pept. Sci.* **2016**, *22*, 149-155.

[16] N. Geudens, M. De Vleeschouwer, K. Feher, H. Rokni-Zadeh, M. G. Ghequire, A. Madder, R. De Mot, J. C. Martins, D. Sinnaeve, *ChemBioChem* **2014**, *15*, 2736-2746.

[17] aN. Geudens, B. Kovacs, D. Sinnaeve, F. E. Oni, M. Höfte, J. C. Martins, *Molecules* **2019**, *24*; bN. Geudens, M. N. Nasir, J. M. Crowet, J. M. Raaijmakers, K. Feher, T. Coenye, J. C. Martins, L. Lins, D. Sinnaeve, M. Deleu, *Biochim. Biophys. Acta - Biomembranes* **2017**, *1859*, 331-339.

[18] I. Kuiper, E. L. Lagendijk, R. Pickford, J. P. Derrick, G. E. M. Lamers, J. E. Thomas-Oates, B. J. J. Lugtenberg, G. V. Bloemberg, *Mol. Microbiol.* **2003**, *51*, 97-113.

[19] J. Gerard, T. Barsby, P. Haden, M. T. Kelly, R. J. Anderson, *J. Nat. Prod.* **1997**, *60*, 223-229.

[20] F. E. Oni, N. Geudens, J. T. Onyeka, O. F. Olorunleke, A. E. Salami, O. O. Omoboye, A. A. Arias, A. Adiobo, S. De Neve, M. Ongena, J. C. Martins, M. Höfte, *Environ. Microbiol.* **2020**, *22*, 5137-5155.

[21] J. F. Dubern, E. R. Coppoolse, W. J. Stiekema, G. V. Bloemberg, *Microbiology (Reading)* **2008**, *154*, 2070-2083.

[22] aS. Dekimpe, J. Masschelein, *Natural Product Reports* **2021**, *38*, 1910-1937; bM. J. Wheadon, C. A. Townsend, *Proc Natl Acad Sci U S A* **2021**, *118*.

[23] F. E. Oni, N. Geudens, O. O. Omoboye, L. Bertier, H. G. K. Hua, A. Adiobo, D. Sinnaeve, J. C. Martins, M. Höfte, *Environ. Microbiol.* **2019**.

[24] W. Li, H. Rokni-Zadeh, M. De Vleeschouwer, M. G. Ghequire, D. Sinnaeve, G. L. Xie, J. Rozenski, A. Madder, J. C. Martins, R. De Mot, *PLoS One* **2013**, *8*, e62946.

[25] L. D. Lopes, E. W. Davis, 2nd, E. S. M. C. Pereira, A. J. Weisberg, L. Bresciani, J. H. Chang, J. E. Loper, F. D. Andreote, *Environ. Microbiol.* **2018**, *20*, 62-74.